

# Supporting Information

**Enhanced photoelectrochemical water splitting performance on TiO<sub>2</sub>  
nanotube arrays coated with an ultrathin Nitrogen-doped carbon  
film by molecular layer deposition\* \***

*Xili Tong, †\*Peng Yang, † Yunwei Wang, † Yong Qin, †\* and Xiangyun Guo<sup>†</sup>*

<sup>†</sup>State Key Laboratory of Coal Conversion, Institute of Coal Chemistry, Chinese  
Academy of Sciences, Taiyuan, 030001, P. R. China.

\*Corresponding Author: [tongxili@sxicc.ac.cn](mailto:tongxili@sxicc.ac.cn) [qinyong@sxicc.ac.cn](mailto:qinyong@sxicc.ac.cn);

## 1. Surface analyses of pristine TNTAs

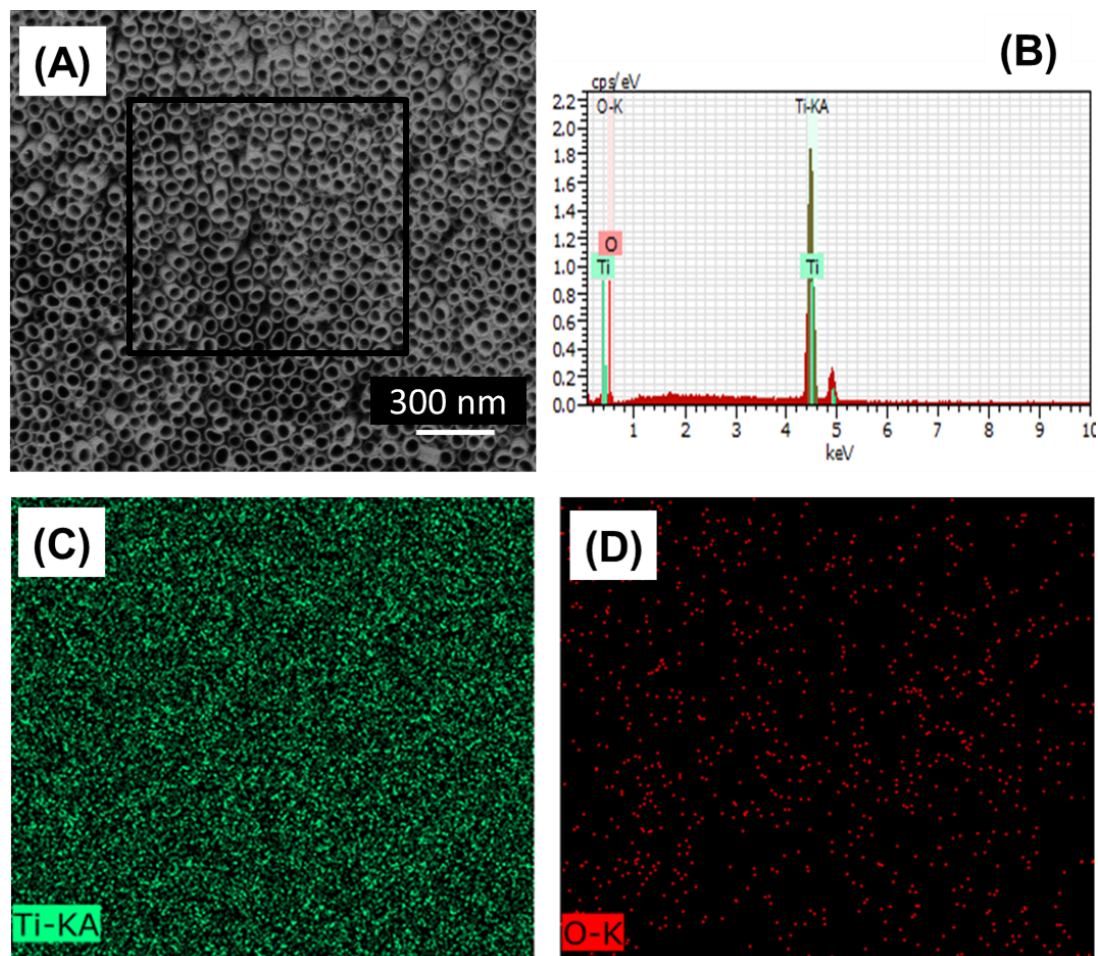


**Figure S1** Element analysis of a pristine TNTAs, (A) the FE-SEM and (B) EDX image of the modified TNTAs. (C-D) Elemental maps of the boxed area in (A) for Ti, and O element, respectively.

In the SEM image of pristine TNTAs, well-aligned NTs vertically oriented from the Ti foil substrate are observed. And only Ti and O elements are detectable by EDX and element map analyses. These results indicate that there are only Ti and O elements in pristine TNTAs, no other elements.

## 2. X-ray photoelectron spectroscopy (XPS) analyses of carbon on Si wafer

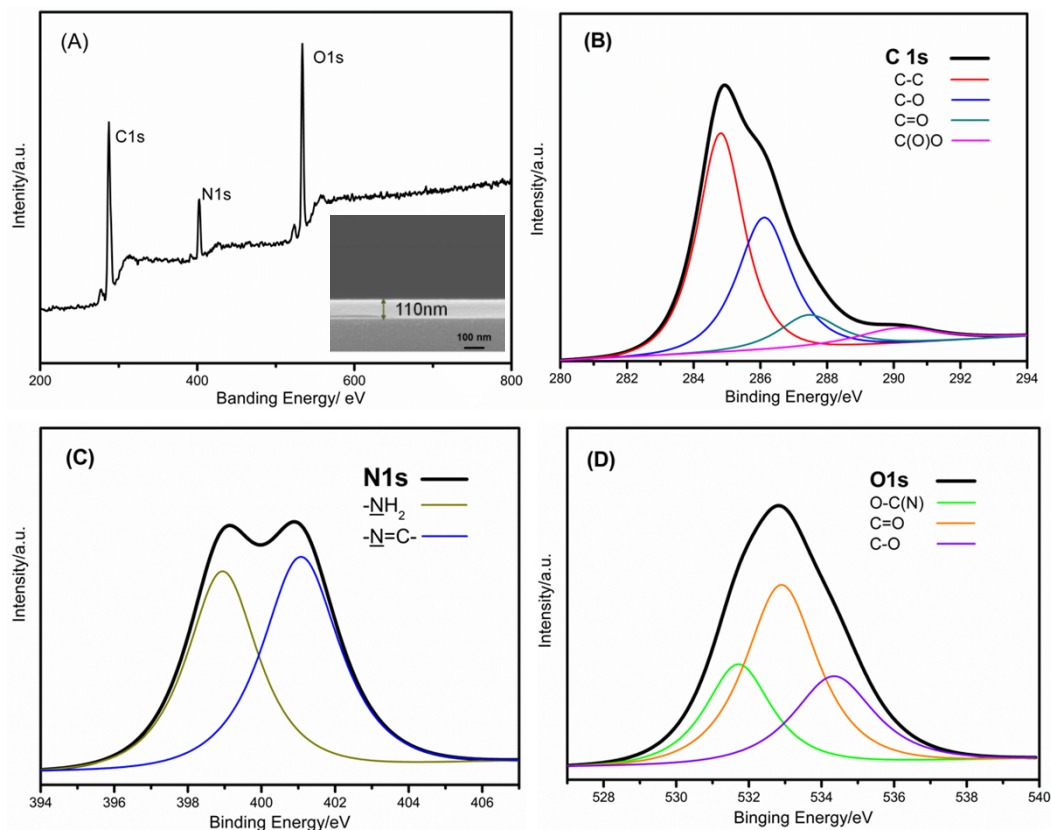


**Figure S2** XPS spectroscopy of (A) the obtained carbon layer on Si substrate with 800 MLD cycles (insert shows the SEM image) (B-D) C<sub>1s</sub>, N<sub>1s</sub> and O<sub>1s</sub> in the obtained carbon layer.

Due to the complete nanostructure of TNTAs, it is inappropriate to analyze the surface composition of carbon layer deposited on TNTAs's walls via MLD using the XPS spectrum. Here, we deposit carbon layer on Si plate not TNTAs with the same MLD method for the accurate XPS analysis of the obtained carbon layer. The morphology of carbon layer on Si substrate displays in the inset of Figure S2A. The cross-section of carbon layer is much flat and regular, and the thickness is about 110 nm. Accordingly, the growth rate of carbon layer is calculated to be 1.375 Å per MLD cycle. Three peaks corresponding to C<sub>1s</sub>, N<sub>1s</sub> and O<sub>1s</sub> are observed near 290.0, 400.0 and 540 eV, respectively (Figure S3A). The contents of C, O and N are measured to be 81.49%, 13.79% and 4.72%, respectively. The C 1s peak in the XPS spectrum shows the presence of four types of carbon bonds, that is, the non-oxygenated ring C (284.5 eV, C-C/ C=C), the C-O (286.5 eV), the carbonyl C in C=O (287.8 eV) and the carboxylate carbon in O=C-O- (290.5 eV) (Figure S2B)[1]. The N<sub>1s</sub> peak shows the presence of two types of nitrogen bonds, that is, pyridine N (398.2 eV) and pyridone N (400.6 eV) (Figure S2C)[2]. The O<sub>1s</sub> peak shows the

presence of three types of oxygen bonds, that is assigned to O=C–N (531.6 eV), C=O (532.8 eV), and C–O (534.4 eV) species, respectively. (Figure S2D)[3] .

### 3, Transmission Electron Microscopy (TEM)

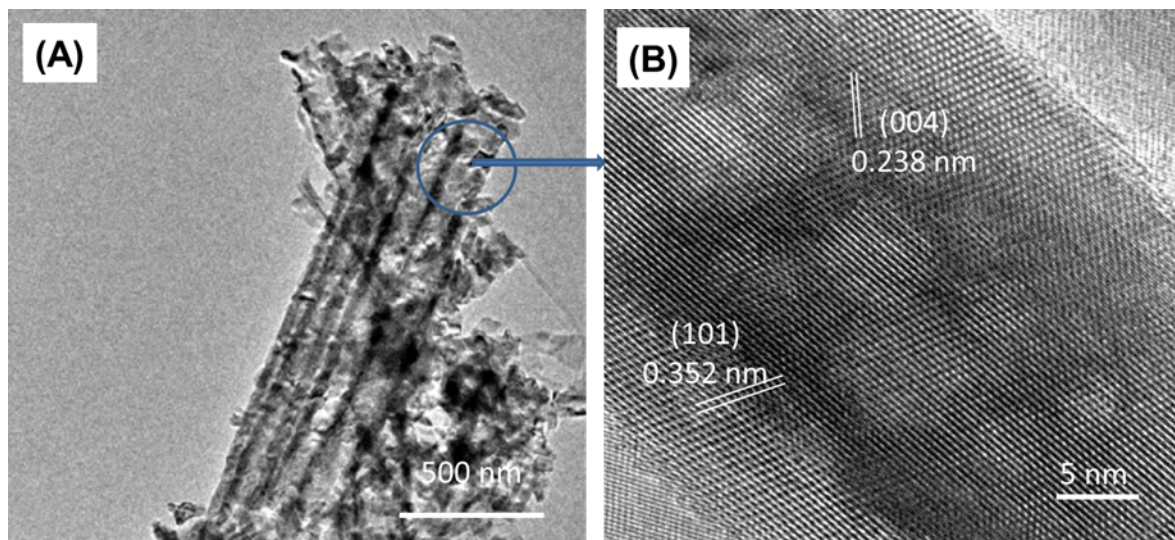


**Figure S3** TEM(A) and HRTEM (B) images of pristine TiO<sub>2</sub>

The TiO<sub>2</sub> NTs were removed from Ti foil with hand scraper, then dispersed in absolute ethanol under sonication for 2 min. A 10  $\mu$ L aliquot of the suspension was dropped onto a carbon-coated copper grid. After 2 min. the excess liquid was removed with filter paper and the sample was air-dried. Figure S3A shows that the nanostructures have uniform diameters of about 90 nm throughout their lengths. HRTEM image (Figure S3B) shows the interplanar spacing of 3.52  $\text{\AA}$  and 2.38  $\text{\AA}$  matches well the (101) and (004) plane of anatase TiO<sub>2</sub>(JCPDS 89-4921), and no carbon layer exists on the surfaces of TiO<sub>2</sub> NTs.

#### 4, HRTEM of modified TNTAs with carbon layer for 5 MLD cycles

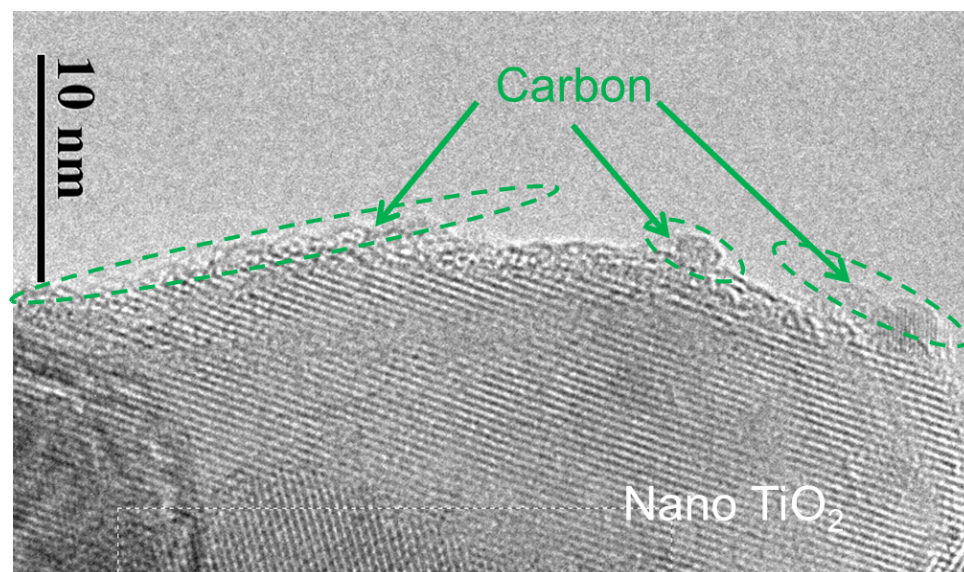


**Figure S4** HRTEM image of the exterior sidewall of TiO<sub>2</sub> nanotube modified with carbon layer for 5 MLD cycles

Figure S4 presents HPTEM image of modified TiO<sub>2</sub> Nanotubes with carbon layers for five MLD cycles. It is observed that carbon film was deposited on the outer sidewall of TiO<sub>2</sub> nanotubes. However, carbon films don't cover the entire outer sidewall. This phenomenon is related to the fact that the thickness of polyimide film synthesized for five MLD cycles is so thin that some cracks will appear when polyimide undergoes the carbonization at high temperature. Therefore, the obtained carbon films under this condition can't effectively prohibit the electrolyte or air from contacting the surface of modified TNTAs.

## 5.XRD measurement

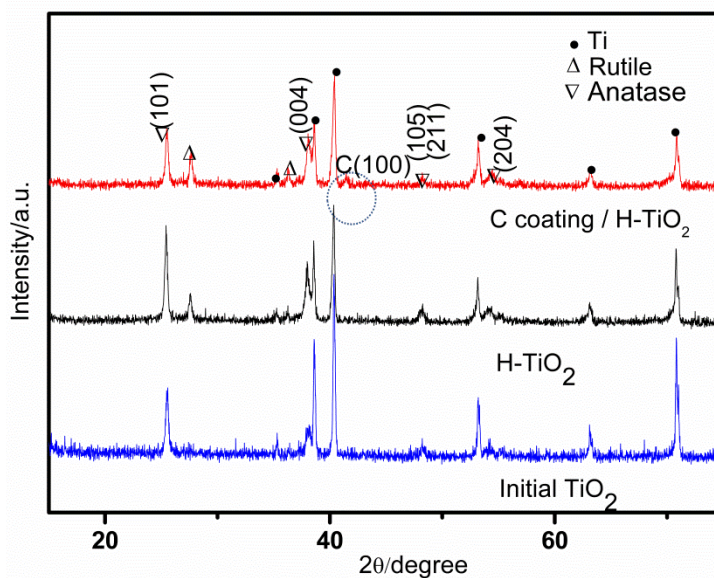


**Figure S5** XRD pattern of Initial TiO<sub>2</sub> (blue line), H-TiO<sub>2</sub> (black) and C coating/H-TiO<sub>2</sub> (red line).

The X-ray diffraction (XRD) pattern in Figure S5 shows that the as-synthesized TNTAs are anatase TiO<sub>2</sub> (JCPDS 89-4921). However, the rutile phase (with respect to the rutile (110) ) peak emerges in the X-ray diffraction pattern of H-TiO<sub>2</sub> and C coating/H-TiO<sub>2</sub> cases due to heat-treatment at high temperature. And the relative intensity of the rutile (110) peak, with respect to the anatase (101) peak, is low, which indicates that most of TiO<sub>2</sub> is still anatase in H-TiO<sub>2</sub> and C coating/H-TiO<sub>2</sub> cases. In addition, the diffraction peaks, at  $2\theta$  of 42.1° corresponded to the graphite crystal face of (100) was detectable only in C coating/H-TiO<sub>2</sub> case, demonstrating that the obtained carbon layer by MLD and followed heat-treatment is well graphitization.

## 6. Electrochemical reaction

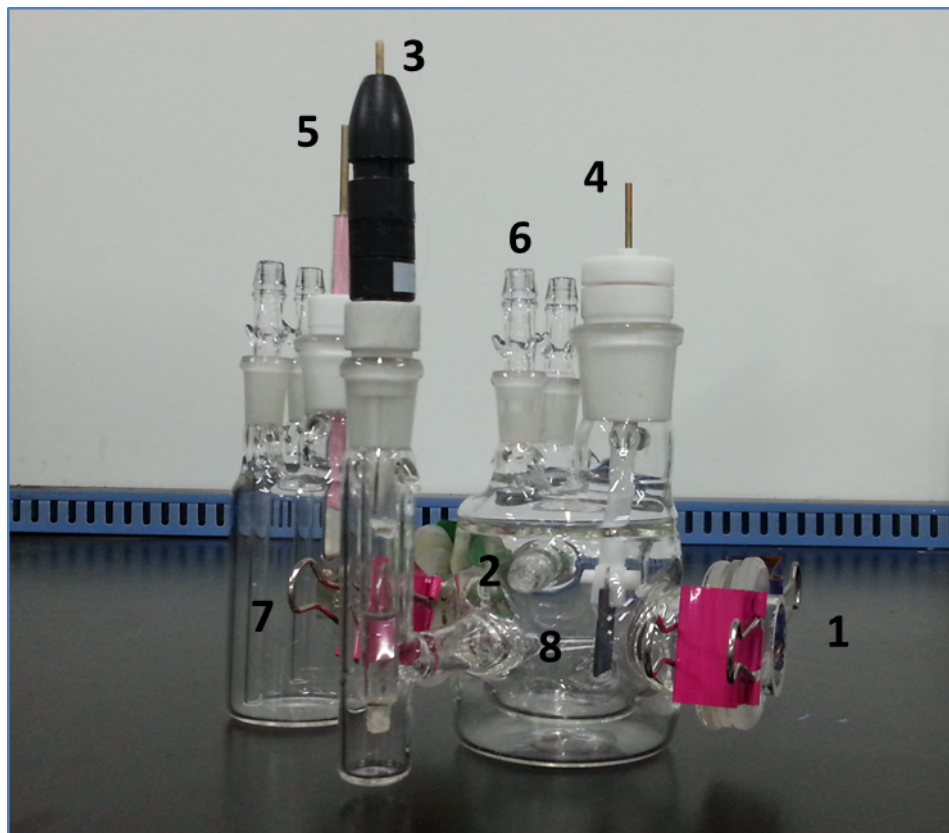


**Figure S6.** Photograph of the electrochemical cell composed of three chambers. (1)the window for light; (2) the inset for cooling water; (3) An Ag/AgCl electrode in  $3 \text{ mol L}^{-1}$  KCl solution (with a nominal potential of 0.210 V versus reversible hydrogen electrode);(4) the working electrode is a  $2 \text{ cm} \times 1.5 \text{ cm}$   $\text{TiO}_2/\text{Ti}$  electrode. Typically, a  $1.5 \text{ cm} \times 1.5 \text{ cm}$  substrate is immersed in the solution;(5) a platinum plate ( $1.5 \text{ cm} \times 1.5 \text{ cm}$ ) is used as the counter electrode; (6) the inset for the gas; (7) a Nafion film; (8) a Luggin capillary separates the working compartment from the reference compartment.

## 7. SEM morphology analyses

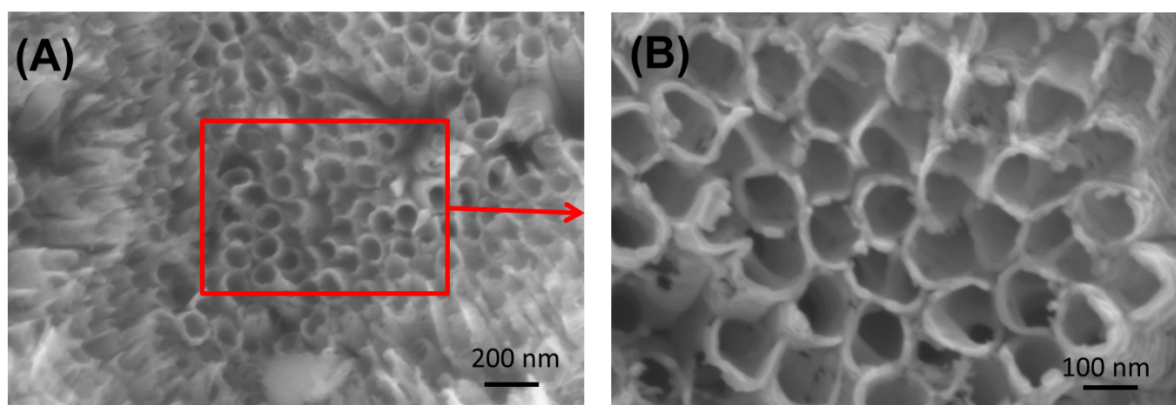


**Figure S7** SEM pattern of Hydrogen treated TNTAs at 600°C, (B) Image of the boxed region in (A) at higher magnification

The anatase-to-rutile transformation has taken place near 600 °C for the 500 nm long nanotubes according to El-Sayed's report of [4]. And the disordered outer layer surrounding the walls of NTs will be formed in the process of hydrogenation, especially at high temperature[5]. Therefore, the structural collapse of some portions of NTs in H-TiO<sub>2</sub> case are observed in Figure S7, indicating that the walls of H-TiO<sub>2</sub> is of high instability. However, this phenomenon hasn't happened in C coating/H-TiO<sub>2</sub> case possibly due to the existence of carbon coating.

## 8, Electrochemical impedance analyses

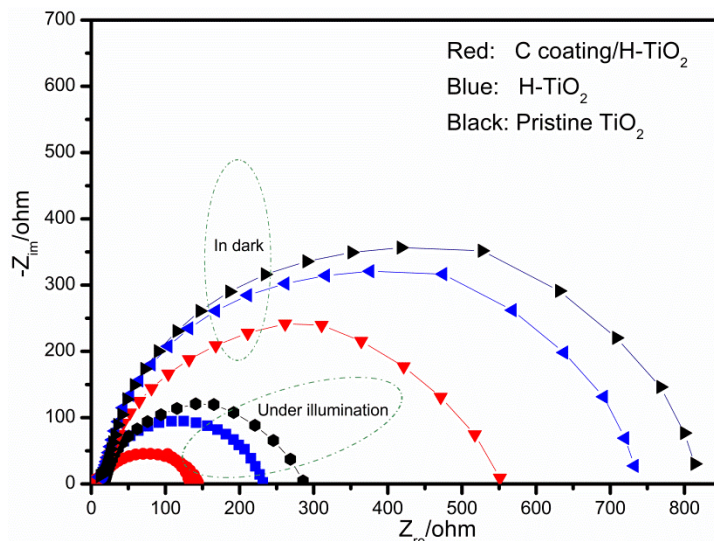


**Figure S8**, Electrochemical impedance spectroscopy of Nyquist plots at an applied potential of 0.23 V vs AgCl/Ag under 100 mW cm<sup>-2</sup> illumination of pristine TiO<sub>2</sub> (black line), H-TiO<sub>2</sub> (blue line) and C coating/H-TiO<sub>2</sub> (red line).

Figure S8 presents Nyquist plots for three samples in dark and under illumination. The diameter of the semicircle is equal to the charge transfer resistance ( $R_{ct}$ )[6]. Three samples all showed lower  $R_{ct}$  value in illumination as compared to those in dark, demonstrating the high photoresponse for three samples.

## Reference

- [1], Akhavan, O.; Abdolhad, M.; Esfandiar, A.; Mohatashamifar, M. *J. Phys. Chem. C* **2010**, *114*, 12955.
- [2], Raymundo Pinero, E.; Cazorla Amoros, D.; Linares Solano, A.; Find, J.; Wild, U.; Schlogl, R. *Carbon* **2002**, *40*, 597.
- [3], Shao, Y.; Zhang, S.; Engelhard, M. H.; Li, G.; Shao, G.; Wang, Y.; Liu, J.; Aksay, I. A.; Lin, Y. *J. Mater. Chem.* **2010**, *20*, 7491.
- [4], Allam, N.K.; El-Sayed, M.A. *J. Phys. Chem. C* **2010**, *114*, 12024.
- [5], Chen, X.; Liu, L.; Yu, P.Y.; Mao, S.S. *Science*, **2011**, 331.746.
- [6], Wen, Z.; Cui, S.; Pu, H.; Mao, S.; Yu, K.; Feng, X.; Chen, J. *Adv. Mater.* **2011**, *23*, 5445.